

DESIGN, FABRICATION, AND CHARACTERIZATION OF AN ACTIVELY-CONTROLLED
MACH 5 TO 8 WIND TUNNEL

A Dissertation Proposal

by

JACOB B. VAUGHN

Submitted to the Graduate and Professional School of
Texas A&M University
in partial fulfillment of the requirements for the degree of
DOCTOR OF PHILOSOPHY

Chair of Committee, Edward White

Committee Members, Rodney Bowersox

Nathan Tichenor

Je Han

Head of Department, Ivett Leyva

March 2024

Major Subject: Aerospace Engineering

Copyright 2024 Jacob B. Vaughn

NOMENCLATURE

Acronyms

ACE	Actively Controlled Expansion
CFD	Computational Fluid Dynamics
FEA	Finite Element Analysis
BCDC	Bush Combat Development Complex
NAHL	National Aerothermochemistry and Hypersonics Laboratory
MDOE	Modern Design of Experiments
MW	Machine Works Inc.
FEDC	Fischer Engineering Design Center
PLC	Programmable Logic Controller
MATLAB	Matrix Laboratory

Common Symbols

M	Mach number
Re/m	Unit Reynolds number
P	Pressure
T	Temperature

Greek Symbols

ρ	Density
μ	Dynamic viscosity

Common Subscripts

0	Stagnation condition
---	----------------------

TABLE OF CONTENTS

	Page
NOMENCLATURE	1
TABLE OF CONTENTS	2
LIST OF FIGURES	4
LIST OF TABLES.....	5
1. INTRODUCTION & LITERATURE REVIEW	1
1.1 Introduction.....	1
1.2 Research Outline and Objectives	1
1.3 Literature Review	3
2. DESIGN AND FABRICATION OF ACE2.0	7
2.1 Background and Motivation	7
2.1.1 ACE Turbulent Transition.....	7
2.1.1.1 ACE Nozzle Noise Surveys.....	7
2.1.1.2 Evaluation of Suspect Transition Mechanisms	8
2.1.2 Active Contol Capability	13
2.2 ACE2.0 Design.....	13
2.2.1 Design Requirments	14
2.2.2 Nozzle Contour Codes	15
2.2.3 CFD	18
2.2.4 20-Ton Linear Actuators Design.....	18
2.2.4.1 Nozzle and Settling Chamber Design	19
2.2.4.2 Frame Design	19
2.2.4.3 Actuation System Design	19
2.2.4.4 Final Overall Design	19
2.2.4.5 FEA	19
2.3 Fabrication Plans	19
2.3.1 Pressure Test	20
2.3.2 Polishing	20
2.4 Final Assembly, Installation, and Calibration.....	20
2.4.1 Actuation Homing and Calibration	20
2.4.2 Shakedown and First Runs	20
3. EXPERIMENTAL APPROACH & OBJECTIVES	22

3.1	Experimental Control and Efficiency Improvements	22
3.1.1	Feedback-Controlled Mach Number Selection	22
3.1.2	Reynolds Number Control Scheme	22
3.2	Nozzle Noise and Uniformity Characterization with Hysteresis.....	23
3.2.1	Uncerntainty Quantification.....	24
3.2.2	Hysteresis	25
3.3	Model Flow Characteristics Hysteresis During Mach Trajectory and Oscillation	25
4.	FUTURE WORK.....	27
4.1	Maybe.....	27
4.2	Possibly	27
	REFERENCES	28
	APPENDIX A. FIRST APPENDIX	33
	APPENDIX B. APPENDIX 2	34
B.1	Appendix Section	34
B.2	Another Appendix Section.....	34

LIST OF FIGURES

FIGURE	Page
2.1 ACE freestream pressure fluctuations at nozzle exit (2014)	8
2.2 ACE freestream pressure fluctuations at various locations (2019).....	9
2.3 ACE freestream pressure fluctuations at 6 in. and 17 in. upstream of nozzle exit (2022)	10
2.4 Mushroom vortex formation at sidewalls	11
2.5 Vertical velocity	12
2.6 Mach lines for noise measured at 17" upstream on nozzle exit.	13
2.7 Comparison of ACE (quadratic) and ACE2.0 (quartic) expansion at throat	17
2.8 Mesh in Pointwise for ACE (top) and ACE2.0 (bottom) nozzle contours.....	18
2.9 Temporary full CAD design	21
3.1 Traverse configurations	24
3.2 Pitot probe measuring 17 in. upstream of nozzle exit.	25
3.3 Drawing of 7° half-angle fin-cone model used for heat flux hysteresis study.	26
A.1 A caption here	33
B.1 A caption here	34

LIST OF TABLES

TABLE	Page
2.1 Settling chamber velocities (ft/s) for combinations of settling chamber heights and Mach numbers.	16
3.1 Test matrix for preliminary noise hysteresis in ACE.	24
3.2 Test matrix for ACE2.0 characterization and noise hysteresis study.	26

1. INTRODUCTION & LITERATURE REVIEW

1.1 Introduction

In recent decades, the continual improvement in hypersonic aircraft aerodynamics has emphasized the need for advancements in wind tunnel ground testing capabilities [1]. The conventional approach, reliant on distinct nozzles for discrete Mach numbers, poses logistical challenges and limits the exploration of dynamic characteristics in evolving aircraft designs. Recognizing these limitations, there is a growing demand within the hypersonic community for a novel solution, namely a continuously variable Mach-number nozzle designed to seamlessly adapt to the evolving needs of hypersonic research.

This imperative shift towards innovation seeks to overcome the constraints of conventional wind tunnels by introducing a continuously variable Mach-number nozzle to provide researchers with a more similar representation of real-world scenarios. By dynamically adjusting the Mach number throughout the wind tunnel runs, the variable conditions experienced by hypersonic vehicles during different flight trajectories can be replicated. This capability enables the advancement of ground testing for a more comprehensive understanding of dynamic hypersonic phenomena.

The Actively Controlled Expansion (ACE) wind tunnel at Texas A&M University has served as a workhorse in hypersonic research for over a decade, but it is overdue for improvements to meet the growing demand of hypersonic flight research. Although the facility was initially designed to facilitate the continuous variation of Mach number, the mechanical implementation ultimately proved to be overly simplistic. Consequently, the nozzle predominantly maintained a fixed Mach 6 setting throughout the majority of the tunnel's operation, falling short of fully realizing its designated variable nature.

1.2 Research Outline and Objectives

In order to maintain the National Aerothermochemistry and Hypersonics Laboratory (NAHL) as a cutting-edge research facility, its current facilities are rapidly advancing in capability to en-

able better science. The objectives of this research aim to lay the foundation for variable Mach number wind tunnel control to meet the recent increased demand of dynamic hypersonic vehicle aerodynamics research.

The existing ACE facility will be upgraded to achieve true active control and to potentially produce low-disturbance flow for higher Reynolds numbers. Its successor, ACE2.0, will employ a feedback-control system with servo motors, linear actuators, and various instrumentation to enable the accurate and continuous variation of Mach number and Reynolds number. Once fabricated and calibrated, the ACE2.0 facility will be utilized to accomplish the following objectives:

1. Improved experimental control and efficiency
 - (a) Feedback-controlled active Mach number selection
 - (b) Constant/proportional Reynolds number control
2. Characterization of noise and uniformity throughout nozzle
 - (a) Uncertainty quantification
 - (b) Hysteresis investigation
3. Preliminary investigation of model flow characteristics hysteresis during Mach trajectory and oscillation

These objectives will effectively demonstrate the capabilities and merit of the new ACE2.0 facility. The intent is to evaluate the performance of the facility while paving the groundwork for the next decade of dynamic hypersonic flight research. In addition, the standard operating procedures for ACE2.0 will be updated to reflect the best practices deduced throughout the completion of these objectives, and the resulting control procedures and interface will be straightforward and well documented for future student researches to easily learn and utilize, ensuring a seamless transition for future investigations. The documentation will not only enhance the accessibility of ACE2.0 for subsequent research endeavors but also contribute to the broader scientific community

by providing a robust framework for effective wind tunnel control and dynamic hypersonic vehicle aerodynamics exploration.

1.3 Literature Review

The literature review for this dissertation will be examined in four parts related to hypersonic variable Mach-number wind tunnels and according to the above objectives: (1) variable mach number nozzle design, (2) parameter control, (3) flow characterization and uncerntainty, and (4) hysteresis in hypersonic flows. This review will discuss articles that establish the most current knowledge base and techniques in the relevant areas of hypersonic wind tunnel research.

Variable Mach number nozzles have been explored in many configurations since the 1950s such as interchangeable fixed-block, plug-type, asymmetric sliding blocks, tilting plate, fully flexible, and hinged/flexure [2]. Each of these designs have varying degrees of flow quality, cost effectiveness, and experimental efficiency that must be considered. Only the fully flexible and flexure designs maximize experimental efficiency without sacrificing flow quality. Of these two, the flexure design minimizes costs by reducing mechanical complexity and supporting structure. Therefore, the flexure design is the optimal choice considering these criteria.

The flexure type nozzle was first proposed in 1955 by Rosen [3] and improved upon separately by Erdmann and Rom [4, 5] in order to minimize the mechanical complexity. This simple nozzle design operated by a single jack greatly reduces manufactring and controls costs and allows for greater flexibilty in active control to quickly and continuously vary the Mach number to model dynamic supersonic vehicle flight.

In the last decade, many variable mach number supersonic wind tunnels have been manufactured due to increased demand of hypersonic flight research. The majority of these are fully flexible or flexure nozzle designs with varying implementations of actuation and control [6–12]. All of these facilites were developed to study vehicle flight trajectory and the hysteresis phenomenon therein.

With the increased emergence of these variable mach number facilites, effective control schemes must be employed for the flow paramters M , P_0 , T_0 , and the resulting Re/m in order to vary each

parameter independently and accurately model hypersonic flight conditions through various trajectories by maintaining flow similarity. This control problem, acknowledged as early as the 1980s, prompted the development of diverse solutions implementing the various areas of control theory such as optimal control [13, 14], state feedback control, mathematical model prediction control, preprogrammed controllers [15], and PID control [16, 17].

In recent years, researchers at numerous state-of-the-art variable Mach number facilities have embraced advanced intelligent control methods. Techniques such as fuzzy logic, genetic algorithms, neural networks, adaptive control or gain scheduling, and their combinations have been applied [18, 19], reflecting a contemporary shift towards leveraging intelligent algorithms to address the complexities and nonlinearity of hypersonic wind tunnel flow control. The methods that will be explored in this research are those of Hwang [14], Matsumoto [15], Ilić [17], and Shahrabaki [19] as they each introduce the different advantages and challenges of each control technique.

First, Hwang developed a robust LQG/LTR based controller enhanced by an anti-integrator windup and a modified Smith predictor to overcome unavoidable modeling errors, uncertainties, and time-delay effects. This controller demonstrated a faster stabilization and exhibited fewer oscillations in comparison to its PID counterpart. Given its superior performance, it presents an appealing prospect for implementation in ACE2.0, and a detailed exploration of this controller will be undertaken in a subsequent chapter.

Next, Matsumoto took a simplified approach by replacing an existing real-time PID controller with a preprogrammed controller to avoid input time delays. This was advantageous for his facility because the run time was not much longer than the time delay for the PID controller to stabilize. This is the most straightforward approach to obtain specific constant or dynamic trajectories of multiple input parameters, but it is not without its challenges. The controller must have a new program for each individual desired parameter set condition or path, and each program must be iterated to minimize errors. Additionally, considering the longer run times of ACE2.0, a PID controller has ample time to stabilize and can be implemented.

Then, Ilić implemented a cascade nonlinear feedforward-feedback PID controller as a com-

bined system to enhance a standard single-loop PID. The systems setpoint reference tracking is improved by the feedforward-feedback architecture, and the distrubance rejection is improved by the cascade architecture. With these two architectures combined in one multi-loop controller, large transient overshoots are eliminated, setpoint settling times are decreased, and the overall accuracy of the controlled parameters is maximized. Once again, the improved performance of this controller makes it another appealing prospect for ACE2.0, which will be discussed later.

Lastly, Shahrababaki utilized an artificial neural network and fuzzy logic to enhance a conventional PD controller to handle the complex nonlinearity of the variable mach number wind tunnel flow parameters. The advantages of fuzzy logic include its simplicity and adaptability of introducing new control rules to handle imprecise data, uncertainty, and unmodeled dynamics. The combined advantage that Shahrababaki explores pertains to the utilization of the neural network to develop the membership functions for the fuzzy logic controller. He designed and trained a feed-forward multilayer perceptron neural network according to the database from the mathematical model of the wind tunnel behavior in order to develop the optimal membership functions. This method will only be explored further for ACE2.0 if the methods of Hwang or Ilić do not yield sufficient performance.

Additionally, with parameter control introduced in a hypersonic wind tunnel, the uncerntainty of the various flow parameters can be quantified more effectively. The primary references for the uncerntainty quantification in this research will be the NASA report by Stephens [20] and Hubbard, Chair of AIAA Wind Tunnel Measurement Uncerntainty Committee on Standards, and the dissertation by Curriston in 2024 [21]. The methodology in this report combines the techinques of the prevelant literature on the subject from the last few decades, and Curriston demonstrates this methodolg in essentially a case study for reference.

Now, considering flow characterization in literature, the primary references will be the recent AIAA articles by Chou [22] and Duan [23] on hypersonic wind tunnel freestream disturbance measurements as they clearly provide the latest measurement processes and procedures and reference over 50 publications on relevant topics from the last couple decades. In addition to these two refer-

ences, a decade of NAHL experience and best practices will guide the characterization of ACE2.0 upon its fabrication and initial shakedown.

Finally, the review of hypersonic flow hysteresis in literature yielded many publications discussing the phenomenon primarily in shock interactions and inlet start/unstart processes. The inlet literature will not be referenced directly in this work, but it will undoubtedly be invaluable for future research in ACE2.0. Focusing on the shock interactiions, both numerical and experimental data is presented throughout this literature. Hysteresis has been reported in hypersonic wind tunnel experiments as early as the 1950s [24, 25]. The test conditions that produced hysteresis were usually avoided in experiments until the 1990s when the phenomona began to be studied directly [6, 26, 27]. Recent literature reveals numerical investigations easily reproduced shock interaction hysteresis, while experimental investigations proved more difficult to reproduce the hysteresis due to the freestream noise in conventional facilities [7]. Nevertheless, hysteresis was successfully observed experimentally in low-noise (quiet) wind tunnels [28–30]. Methodolgies from all of this lierature will be studied in order to attempt to reproduce shock interaction hysteresis in ACE2.0. Additionally, the data gathered by Wirth [31] in the existing ACE facility will serve as the primary reference for the exploration of surface heat flux hysteresis of a fin-cone model.

Something about modern design of experiemtns (MDOE) here with reference to DeLoach.

2. DESIGN AND FABRICATION OF ACE2.0

2.1 Background and Motivation

The existing ACE (Actively Controlled Expansion) tunnel was designed and manufactured between 2009 and 2010 and began operating in 2010 [32–34]. The ACE tunnel nozzle is 40 inches long from the throat to the test-section entrance. The test section is 14 inches wide and 9 inches tall. By varying throat height, the test-section Mach number can be varied from $M = 5$ to 8 .

2.1.1 ACE Turbulent Transition

Below a unit Reynolds number of $Re/m = U/\nu \approx 3 \times 10^6 m^{-1}$ the rms pressure fluctuations in the test section are low, less than 1%. At higher Re/m values, pressure fluctuation levels increase when the unit Reynolds number increases above $Re/m \approx 3 \times 10^6 m^{-1}$ [35]. It is desired to increase the unit Reynolds number at which laminar flow can be maintained. This document summarizes the hypothesis and supporting data regarding the pressure fluctuation levels increase and how it might be delayed to higher unit Reynolds numbers. More stuff

2.1.1.1 ACE Nozzle Noise Surveys

Three recent pitot surveys have been conducted in the ACE tunnel. The first by Mai (2014) revealed transition occurring around a unit Reynolds number of $3 \times 10^6 m^{-1}$, as shown in Figure 2.1. The same result was found by Neel (2019) shown in Figure 2.2 that transition occurs at this unit Reynolds number 6 inches upstream of the test section entrance. A final pitot survey in ACE by Wirth (2022) was conducted to determine whether the pressure fluctuation levels increase occurred at different Re/m values at positions farther upstream in the nozzle. He found pressure fluctuation levels increase at $Re' \approx 3 \times 10^6 m^{-1}$ at a measurement location 17 inches upstream of the test section entrance. His results in Figure 2.3 align perfectly with Mai and Neel and clearly establish that the Reynolds number at which pressure fluctuation levels increase is not sensitive to location in the nozzle. This suggests that transition is not moving upstream through the nozzle as Reynolds number is increased.

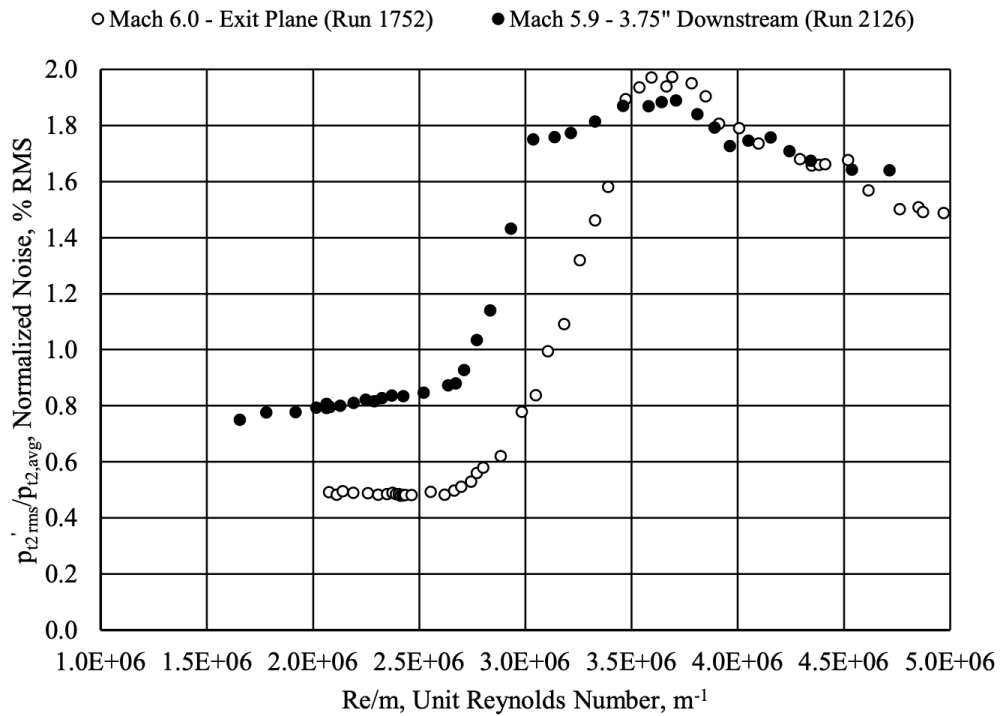


Figure 55. ACE tunnel freestream flow noise at nozzle exit plane and 95 mm (3.75 in.) downstream.

Figure 2.1: ACE freestream pressure fluctuations at nozzle exit (2014) [36]

2.1.1.2 Evaluation of Suspect Transition Mechanisms

There are five primary suspects for this transition:

1. A known manufacturing surface discontinuity at the throat
2. Sidewall mushroom vortices
3. Görtler vortices
4. Freestream turbulence in the incoming flow and/or upstream boundary layer
5. Wall roughness or waviness

This following evaluates each of these possibilities and concludes that the primary culprit is

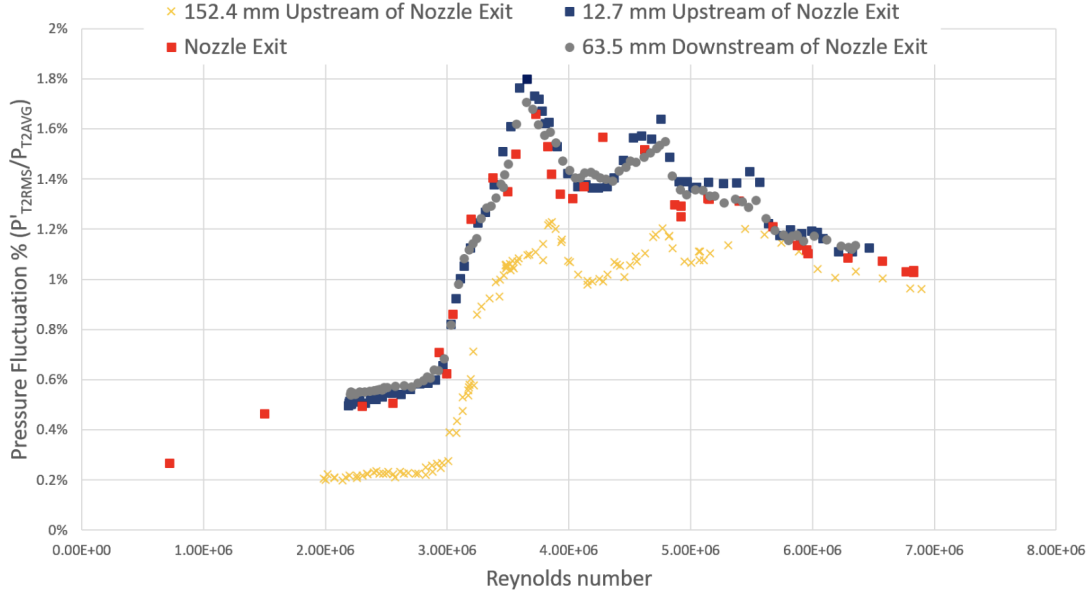


Figure 5.1: Freestream pitot pressure fluctuation levels. ACE tunnel.

Figure 2.2: ACE freestream pressure fluctuations at various locations (2019) [37]

the surface discontinuity at the throat. This conclusion is supported by pitot surveys, method-of-characteristics line tracing, and CFD simulations. Sidewall mushroom vortices and Görtler vortices would lead to transition too far downstream from the throat to be responsible for the pressure fluctuation levels increase. Items 4 and 5 are potential causes of poor flow quality in all supersonic tunnels and are included for completeness. The specific mechanism by which these would cause transition is not known. While they are not the primary suspects for the pressure fluctuation levels increase, improving these conditions will be addressed in the redesign intended to extend laminar flow to higher Reynolds numbers.

Mach Line Tracing

The origin of the noise measured farthest upstream of the nozzle exit was determined by tracing characteristics from the measurement location at the centerline upstream to the wall. Both the side view and top view of this can be seen in Figure 2.6.

The above results reveal the pressure fluctuation levels increase but not the transition mech-

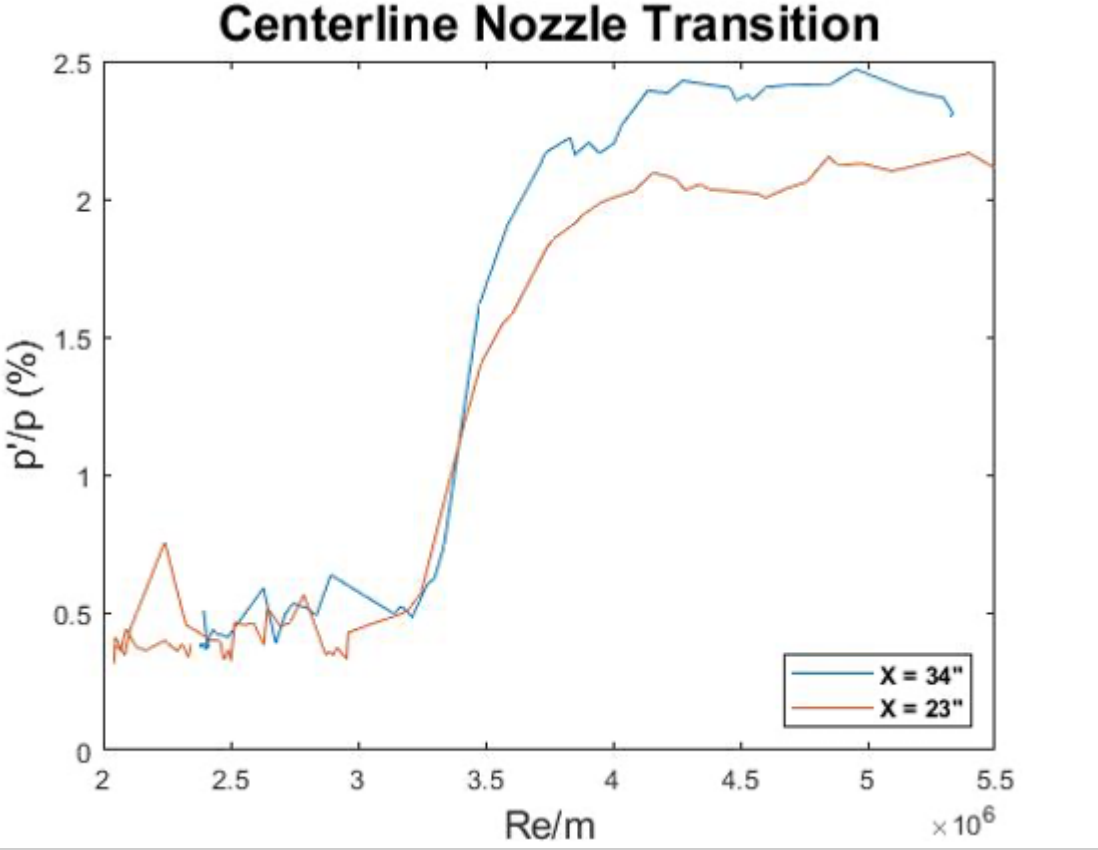


Figure 2.3: ACE freestream pressure fluctuations at 6 in. and 17 in. upstream of nozzle exit (2022)

anism. The two primary suspects that can be eliminated using the data above are the sidewall mushroom vortices and Görtler vortices.

Sidewall mushroom vortices arise from the pressure distribution in the nozzle and the low momentum flow in the sidewall boundary layers. The flow at the centerline expands to the test section pressure ahead of the top and bottom curved walls. The flow at the top and bottom lags behind the centerline flow with a higher pressure to create a vertical pressure gradient that introduces a secondary vertical flow in the sidewall boundary layers that flows from the corners to the centerline [38]. CFD simulations show the sidewall mushroom vortices beginning to form approximately 24 inches upstream of the nozzle exit shown in Figures 2.4 and 2.5. Tracing the characteristics from 17 inches upstream of the test section entrance, Figure 2.6 shows the origin to be upstream of the throat where sidewall mushroom vortices are not relevant.

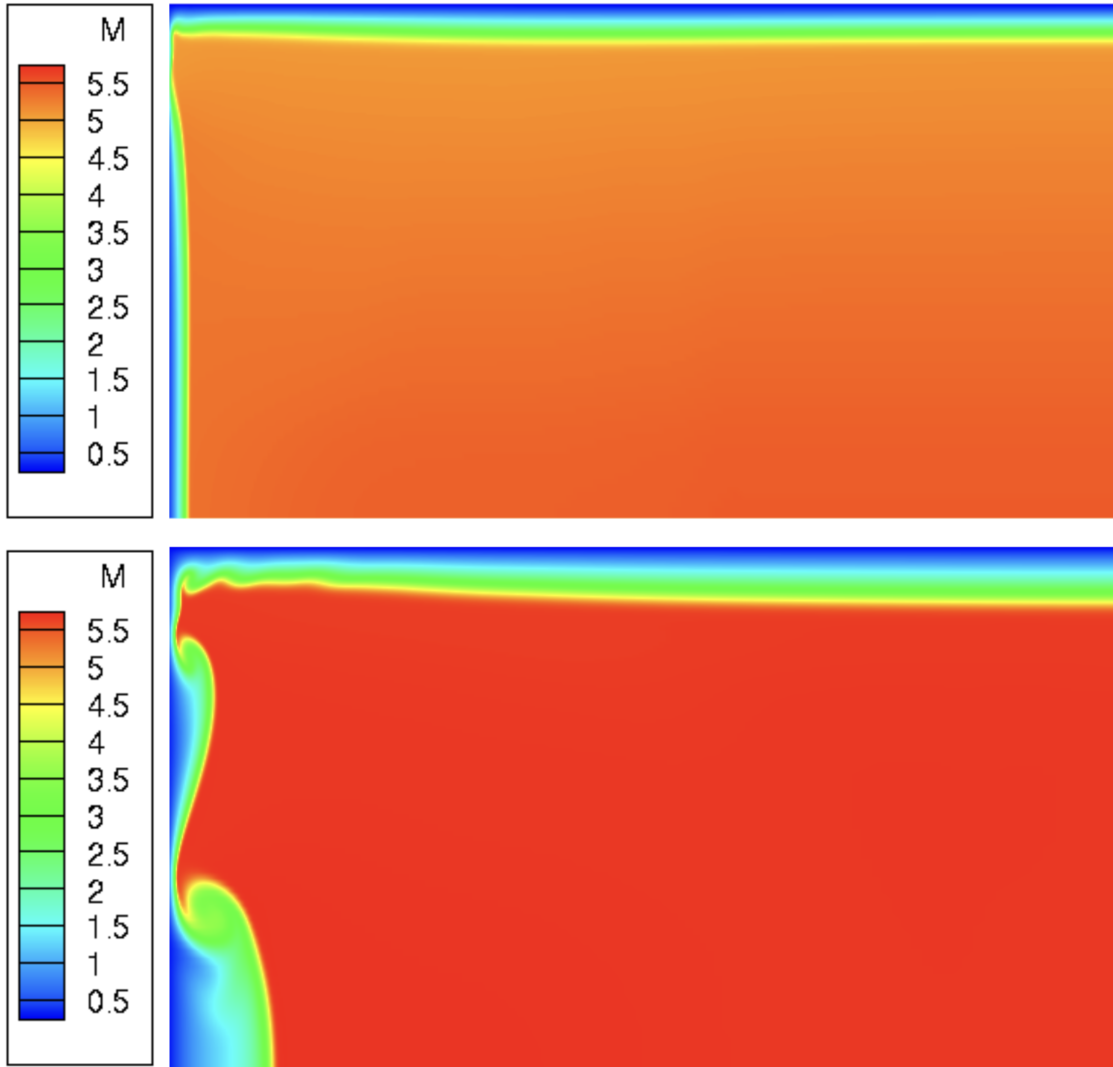


Figure 2.4: Mushroom vortex formation at sidewalls

Görtler vortices are counter-rotating streamwise vortices that occur in boundary layers on concave surfaces [39]. To estimate where these may lead to transition, a CFD basic state simulation and N-factor analysis was performed by Kocian (2022). However, tracing the characteristics from 17 inches upstream of the test section entrance, Figure 2.6 shows the measured noise originates at the end of the straight section of the nozzle where Görtler is not relevant.

While both sidewall vortices and Görtler vortices can play some role in transition in planar nozzles, they are no longer considered suspects for the pressure fluctuation levels increase at unit

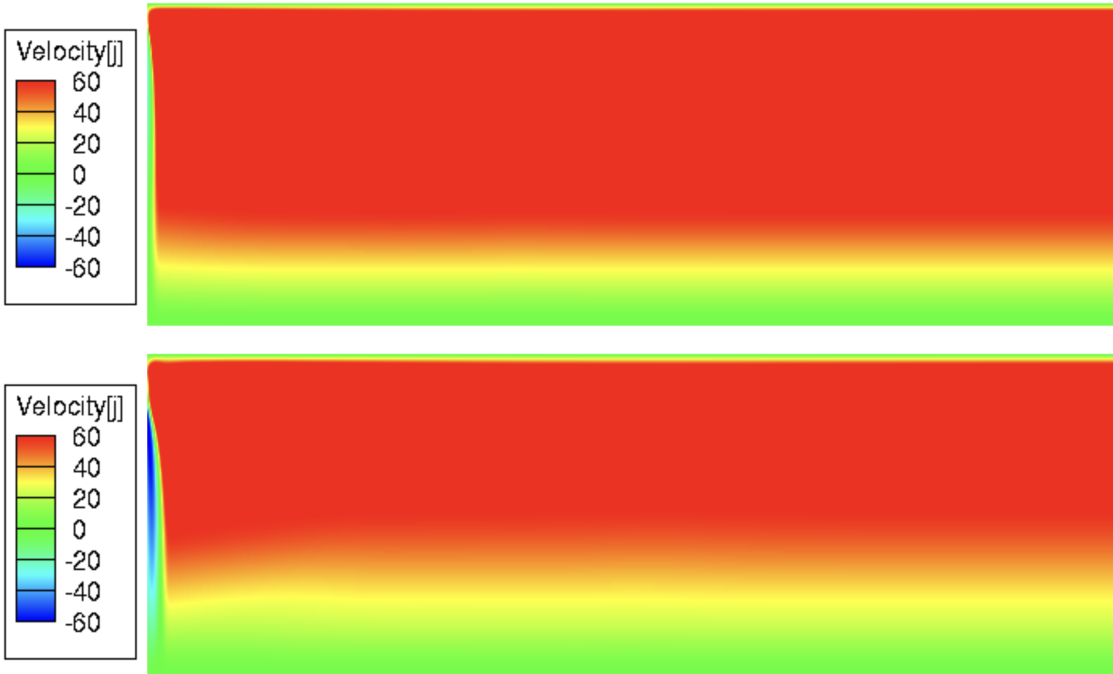


Figure 2.5: Vertical velocity

Reynolds numbers above $3 \times 10^6 m^{-1}$.

The combination of pitot surveys and characteristic tracing eliminates the possibility of side-wall mushroom vortices or Görtler vortices because these instabilities would lead to transition downstream of the characteristic wall origins found by tracing from the measurement location to the wall intersection. This leaves the surface discontinuity at the throat as the primary culprit for the pressure fluctuation levels increase. The remaining suspect mechanisms are still important to note and address in the redesign of the ACE tunnel.

The following improvements are recommended to obtain laminar flow for some value above $Re' \approx 3 \times 10^6 m^{-1}$:

1. Second-derivative-smooth subsonic-to-supersonic throat transition (eliminate discontinuity)
2. Continuous curvature with analytical functions (eliminate waviness and discontinuities)
3. Mirror polishing as much as possible (eliminate roughness/waviness)

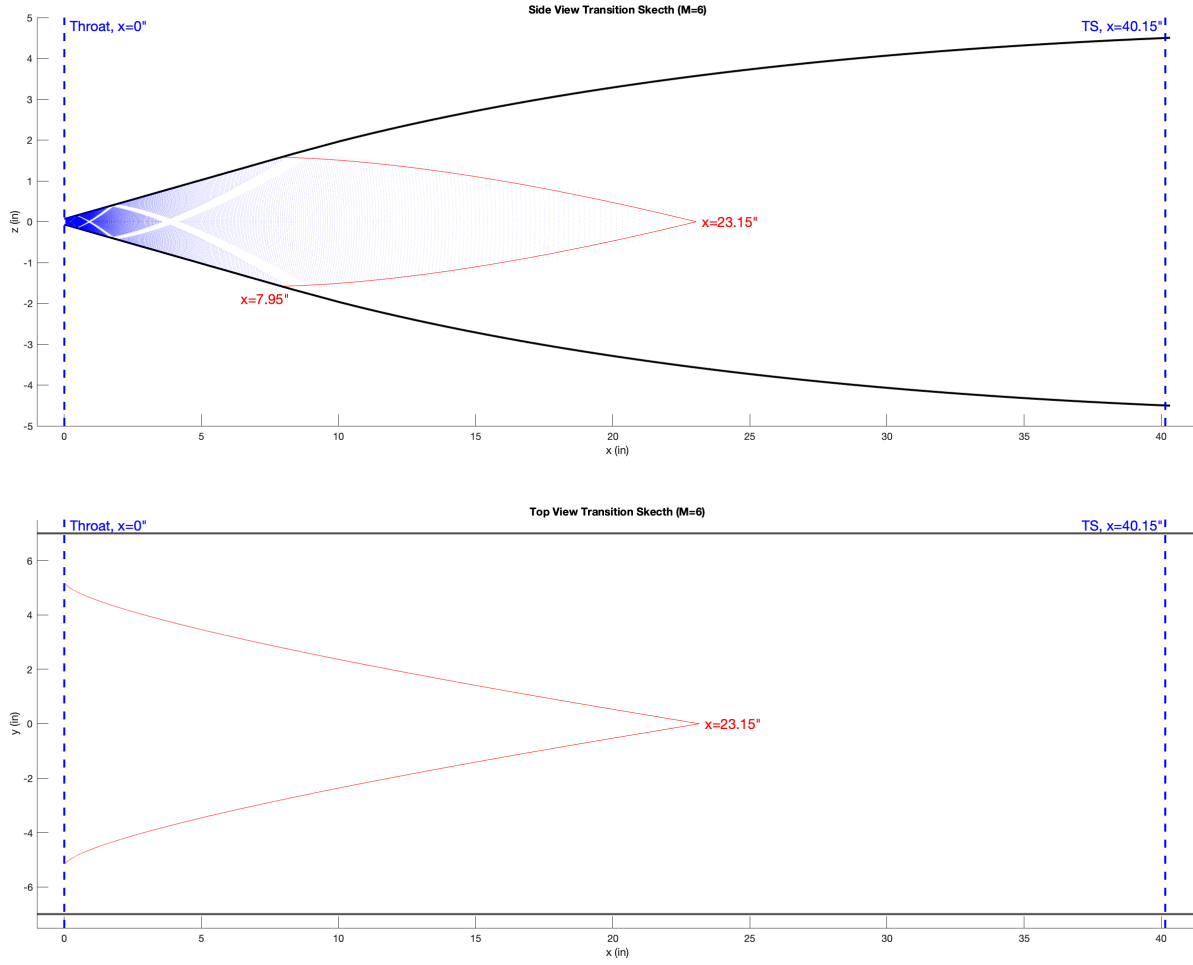


Figure 2.6: Mach lines for noise measured at 17" upstream on nozzle exit.

4. Improved settling chamber performance

5. Subsonic boundary layer suction/bleed

2.1.2 Active Control Capability

Despite the intention of the ACE design, the mechanical realization does not allow for active control. In fact, changing the Mach number at all is far from a simple process.

2.2 ACE2.0 Design

Following the above conclusions and recommendations, the most likely reason the pressure fluctuations increase is laminar-to-turbulent transition due to a surface discontinuity at the throat.

This conclusion is supported by pitot surveys, CFD, and method of characteristics line tracing described above. To correct this, the nozzle will be redesigned and remanufactured to meet specific requirements that will ensure the best performance and potentially expand the laminar Reynolds number range. The decision to remanufacture the nozzle presents an opportunity to revise the nozzle and settling chamber design to achieve true active controllability, properly embodying ACE2.0 name.

The rest of the chapter details the planned improvements to the ACE tunnel and specific design requirements that will achieve those improvements. In addition to a new nozzle, the settling chamber will also be redesigned to improve the uniformity and turbulence of the incoming flow into the nozzle. These improvements are to achieve the goal of increasing the unit Reynolds number at which laminar nozzle flow is maintained.

2.2.1 Design Requirements

ACE2.0 shall maintain many characteristics while improving some, so many requirements are the same as the original ACE design. The new tunnel will still produce uniform Mach 5 to 8 flow in the 9 inches by 14 inches test section, withstand a 530 Kelvin total temperature, and maintain an engineering factor of safety of 4 when operating at a total pressure of 200 psi.

The overall improvements and associated requirements will be a new frame that will support a new actuation system with an efficient means of repeatably adjusting throat height to achieve desired mach numbers with a displacement indicator to achieve a repeatable Mach number change by 2 students in 4 hours or less, straightforward settling chamber and nozzle access for inspection and maintenance, and a rigid assembly for actuation between the settling chamber and nozzle.

Nozzle Requirements

The current ACE nozzle successfully produces uniform Mach 5 to 8 flow in its core. In order to maintain this good performance and not introduce unknown parameters, the new nozzle will retain a very similar contour with slight improvements. The requirements that remain the same are that the nozzle must produce uniform flow for the entire Mach range, achieve maximum height

deflection without damage, and prevent leaks up to a pressure of 200 psi.

The improvements to the nozzle and associated requirements will be a single-piece nozzle that eliminates any potential manufacturing discontinuities or steps, a contour with continuous 1st and 2nd derivatives that is specified by an analytical functions that will eliminate discontinuities and truncation error, and a maximum allowable stress less than or equal to that found in the current ACE flexure.

Settling Chamber Requirements

The current ACE settling chamber design provides multiple opportunities to improve flow conditioning and ease of maintenance. The new settling chamber design will increase the length and height and allow for variable aerogrid/screen configurations. The requirements that remain the same are low freestream turbulence, thin stable wall boundary layers, maximum uniformity, and preventing leaks at a pressure of 200 psi. The implementation of these requirements will be improved in the new design to achieve improved incoming flow into the nozzle.

Following Reshotko [40], the length of the settling chamber shall accommodate a separation of 250 characteristic mesh sizes between screens allowing for adequate turbulence decay. The aerogrids will have a hexagonal perforation pattern to increase porosity and decrease pressure loss. The number of aerogrids and screens shall be variable to allow for future flow conditioning experiments. The inlet shall include a baffle system that will provide an acceptable initial distribution of air received from the high-pressure inlet piping. The overall design shall accommodate future boundary layer suction or bleed slots.

A settling chamber height of 6" was chosen ... 10 ft/s to 100 ft/s Pope [41]:

2.2.2 Nozzle Contour Codes

The method-of-characteristics Fortran script written by Bowersox that produced the ACE nozzle contour was used for the new nozzle contour. In order to achieve continuous first and second derivative continuity, a section of the code was modified to produce a fourth-order expansion section instead of the original second-order curve. This allowed the expansion section to match the

Height	Mach Number			
	5	6	7	8
4"	73.57	34.55	17.64	9.66
5"	58.83	27.64	14.11	7.73
6"	49.01	23.03	11.76	6.44
7"	42.00	19.74	10.08	5.52
8"	36.75	17.27	8.82	4.83
9"	32.66	15.35	7.84	4.29

Table 2.1: Settling chamber velocities (ft/s) for combinations of settling chamber heights and Mach numbers.

curvature of both the subsonic section and the straight section.

Before:

```
do 10 i=1, nch
  theta(i) = dthetai + float(i-1)*dth
  x(i) = tan(theta(i))/2./k
  xw(i) = x(i)
  y(i) = 1.0 + k*x(i)**2
  yw(i) = y(i)
10 continue
```

After:

```
do 10 i=1, nch
  theta(i) = dthetai + float(i-1)*dth
  xthetai = sqrt(tan(thetai)/k)
  k4 = -k/2./xthetai
  pc = -9.*(k**2)/3. /((4.*k4)**2)
  qc = (2.* (3.*k)**3 - 27.*((4.*k4)**2)*tan(theta(i)))
  & /27. /((4.*k4)**3)
  npi = 2.*pi/3.
  tc = 2.*sqrt(-pc/3.)
  & *cos(acos((3.*qc/2./pc)*sqrt(-3./pc))/3. - npi)
  if((3.*qc/2./pc)*sqrt(-3./pc).lt.-1.) then
    tc = 2.*sqrt(-pc/3.)*cos(acos(-1.)/3. - npi)
  end if
  x(i) = tc - k/4./k4
  xw(i) = x(i)
  y(i) = 1.0 + k*x(i)**3 + k4*x(i)**4
  yw(i) = y(i)
10 continue
```

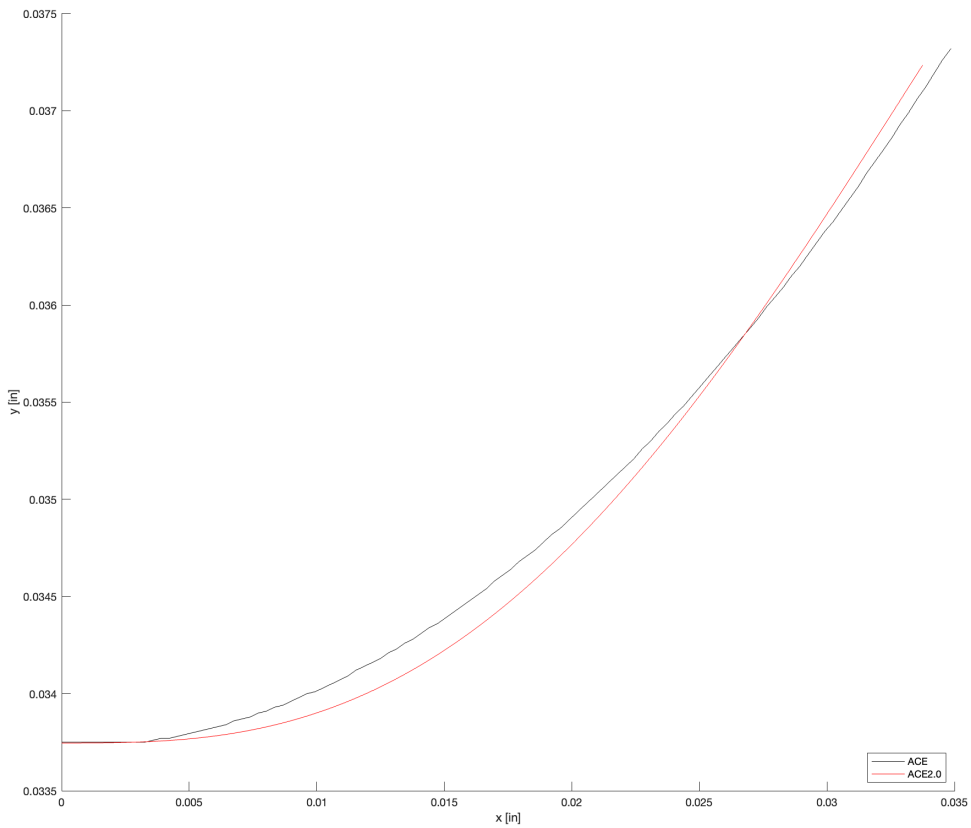


Figure 2.7: Comparison of ACE (quadratic) and ACE2.0 (quartic) expansion at throat

After the points were produced by the Fortran script, they were imported into a MATLAB script to fit with analytic functions.

Equations as follows:

Subsonic: $-0.0002679752287799994x^5 - 0.0066993807195x^4 - 0.04466253813x^3 + 0.033746187$

for $-10 < x < 0$

Throat: $-2689.610971179115x^4 + 181.528229581324x^3 + 0.033746187$ for $0 < x < 0.033746187$

Straight: $0.206725280364801x + 0.030258092015591$ for $0.033746187 < x < 6.1460114$

Straightening: $2.180909737850381x^{0.960492634168194} + 5.934566177927477 \times 10^{284}x^{-367.9331632104439} - 0.585293189697896 - 1.684363604007221x^{1.011336503949665} - 0.023814395465567 \ln(0.418646933043039x)$

for $6.1460114 < x < 40.07774$

2.2.3 CFD

In order to verify the above nozzle contour performance compared to the original ACE contour, both contours were simulated in 2-D with CFD. First, a mesh was created in Pointwise for each contour with 400 equally spaced columns of cells in the x-direction. Each column had the spacing scaled to accurately capture the boundary layer with the smallest cell height around 1e-5 meters at the curved wall and the largest around 0.1 meters at the centerline as seen in Figure 2.8.

After creating a mesh for each, they were ran in US3D on the Texas A&M supercomputer, GRACE. *Stuff about inputs and convergence conditions*

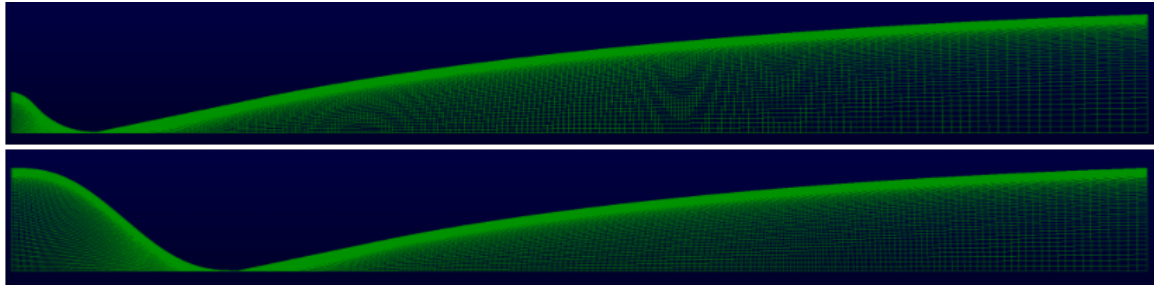


Figure 2.8: Mesh in Pointwise for ACE (top) and ACE2.0 (bottom) nozzle contours

2.2.4 20-Ton Linear Actuators Design

The updated ACE design follows the requirements above and is shown in the following figures. The new design exhibits an improved nozzle contour, settling chamber, and actuation design:

- The overall length was increased by 16 inches to accommodate the much larger settling chamber.
- The actuation design consists of multiple worm gears to achieve a high gear ratio with minimal backlash. The Mach number can be changed quickly and accurately with a 0.005 inch throat height adjustment per control shaft rotation.

- The settling chamber exhibits inlet flow spreaders and an adaptable flow conditioner design.
- The nozzle is a single piece to eliminate any potential manufacturing steps and discontinuities.
- The stand will integrate with existing ACE infrastructure.

2.2.4.1 Nozzle and Settling Chamber Design

The nozzle and settling chamber are combined to accommodate active control.

The flow conditioners will be enclosed in a standalone box that can be modified or replaced easily.

The nozzle blocks will be made from 304 stainless steel, and the flexures will be made from 17-4 PH stainless steel.

2.2.4.2 Frame Design

Stuff and figures

Originally planned to water jet bars from brace stock to save material cost and reduce excess.

Later discovered that the cost of time and tooling on water jet to cut all pieces from 3 inch 4140 allot steel exceeds the cost of ordering bar stock.

2.2.4.3 Actuation System Design

Detailed specifics of actuation components

2.2.4.4 Final Overall Design

Pictured below is the final overall ACE2.0 assembly.

2.2.4.5 FEA

Stress and FOS stuff with figures

2.3 Fabrication Plans

ACE2.0 is currently being fabricated. Most machining is completed. Pictures of machining and fabrication.

2.3.1 Pressure Test

Check structural integrity at 200 psia and evaluate sealing.

2.3.2 Polishing

Astro Pal polishing nozzles and sidewalls to 1 Ra.

2.4 Final Assembly, Installation, and Calibration

The final assembly will occur at NAL. Once nozzles and actuators are assembled in the frame, ACE2.0 will be rolled into the lab to replace ACE. All hoses, wires, and instrumentation attached to the nozzle and settling chamber will be removed and ACE will be rolled out of the lab. ACE2.0 will roll in and reconnect all hoses, wires, and instrumentation.

2.4.1 Actuation Homing and Calibration

Before the sidewalls are installed, the nozzles will be aligned by homing the servo motors with the limit switches. At this point shims will be used to make fine adjustments to limit switch positions to ensure a minimum Mach number of 4.9??? and a maximum Mach number of 8.5???.

2.4.2 Shakedown and First Runs

Decide what the first runs' purposes should be to properly calibrate.

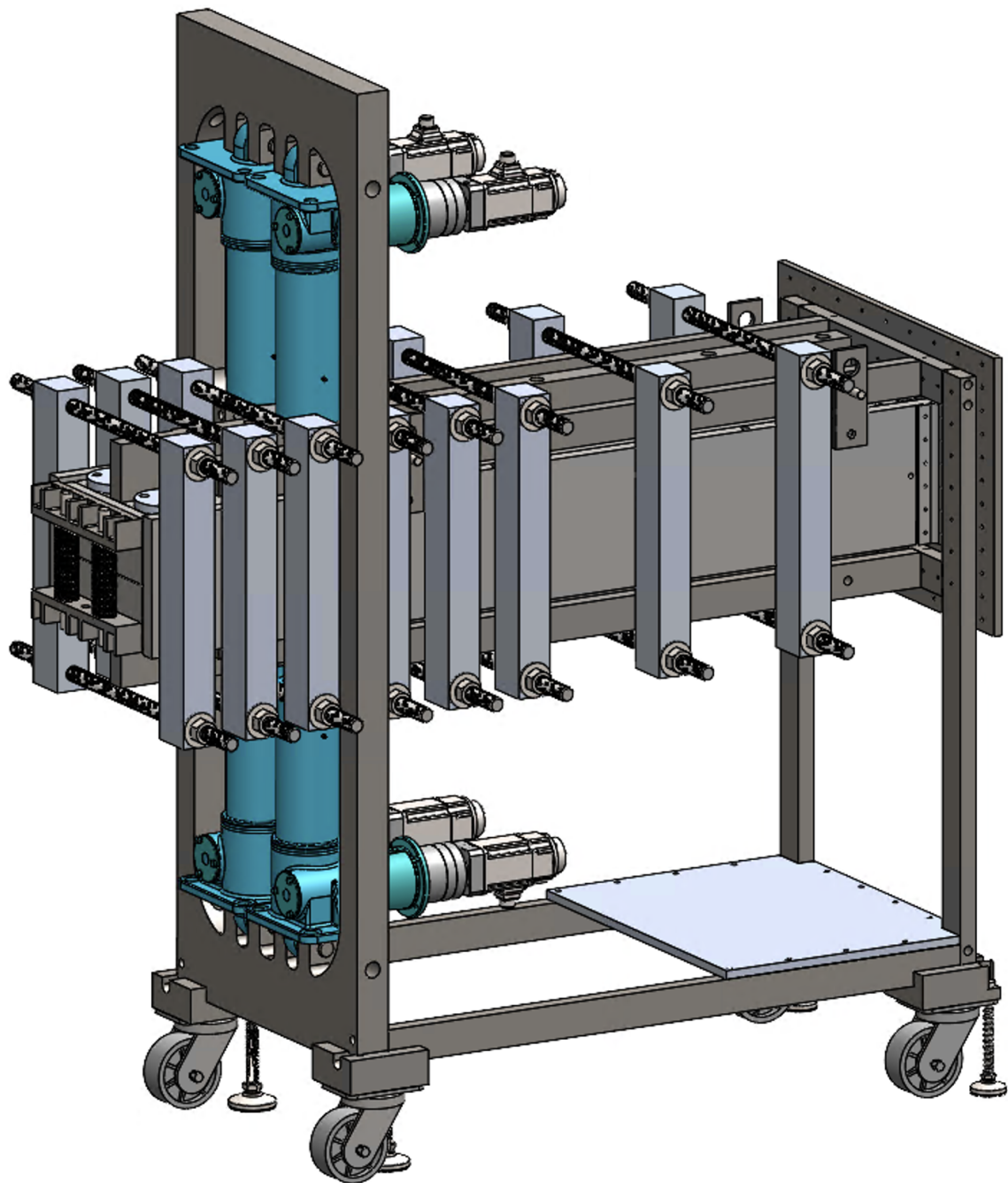


Figure 2.9: Temporary full CAD design

3. EXPERIMENTAL APPROACH & OBJECTIVES

3.1 Experimental Control and Efficiency Improvements

Stuff about ACE2.0 controls

3.1.1 Feedback-Controlled Mach Number Selection

Inputting Mach number into PLC to actively adjust to desired Mach number within some tolerance. Result of above ACE2.0 development.

Unsure how to proceed; review [20].

3.1.2 Reynolds Number Control Scheme

Control P_0 to maintain constant Re/m during Mach sweep. Look into anticipatory change in Re/m for potential delayed response time in P_0 , and look into potential proportional Re/m change to model acceleration or altitude change.

Mathematic model predictive controller or preprogrammed controller will be implemented until an adequate PID controller can be developed.

$$Re/m = \frac{\rho U}{\mu} \quad (3.1)$$

$$\frac{T_0}{T} = \left(1 + \frac{\gamma - 1}{2} M^2\right) = F \quad (3.2)$$

$$\frac{P_0}{P} = \left(1 + \frac{\gamma - 1}{2} M^2\right)^{\frac{1}{\gamma-1}} = F^{\frac{1}{\gamma-1}} \quad (3.3)$$

$$\rho = \frac{P}{RT} = \frac{P_0 F^{\frac{-\gamma}{\gamma-1}}}{RT_0 F^{-1}} = \frac{P_0}{RT_0 F^{\frac{1}{\gamma-1}}} \quad (3.4)$$

$$U = M \sqrt{\gamma RT} = M F^{-\frac{1}{2}} \sqrt{\gamma RT_0} \quad (3.5)$$

$$Re/m = \frac{\rho U}{\mu} = \frac{1}{\mu} \frac{P_0}{RT_0 F^{\frac{1}{\gamma-1}}} M F^{-\frac{1}{2}} \sqrt{\gamma RT_0}$$

$$Re/m = \sqrt{\frac{\gamma}{RT_0}} \frac{M P_0}{\mu} F^{-\frac{\gamma+1}{2(\gamma-1)}} \quad (3.6)$$

For constant Re/m assuming $\gamma, R, T_0 = \text{const.}$ and with $\frac{dF}{dt} = (\gamma - 1)M\frac{dM}{dt}$:

$$\frac{d(Re/m)}{dt} = 0 = P_0 \frac{dM}{dt} + M \frac{dP_0}{dt} - \frac{MP_0}{\mu} \frac{d\mu}{dt} - \frac{\gamma + 1}{2} M^2 P_0 F^{-1} \frac{dM}{dt} \quad (3.7)$$

Sutherland's Law with $T_\mu = 273, S_\mu = 111$, and $\mu_0 = 1.716 \times 10^{-5}$:

$$\mu = \mu_0 \frac{T_\mu + S_\mu}{T + S_\mu} \left(\frac{T}{T_\mu} \right) \quad (3.8)$$

$$\mu = \frac{\mu_0(t_\mu + S_\mu)}{T_\mu^{\frac{3}{2}}} \frac{T_0^{\frac{3}{2}} F^{-\frac{3}{2}}}{T_0 F^{-1} + S_\mu} \quad (3.9)$$

$$\frac{\frac{d\mu}{dt}}{\mu} = (\gamma - 1) M F^{-1} \frac{dM}{dt} \left(\frac{T_0 F^{-1}}{T_0 F^{-1} + S_\mu} - \frac{3}{2} \right) \quad (3.10)$$

Substiuting and solving for $\frac{dP_0}{dt}$:

$$\frac{dP_0}{dt} = P_0 M F^{-1} \frac{dM}{dt} \left[(\gamma - 1) \left(\frac{T_0 F^{-1}}{T_0 F^{-1} + S_\mu} - \frac{3}{2} \right) + \frac{\gamma + 1}{2} - \frac{1}{M^2 F^{-1}} \right] \quad (3.11)$$

While this model is ..., the actual controls may not be physically impleted by the author due to time constraints and the fact that the M6QT shares the air supply controls. Installing controllable valve would disrupt testing in both facilities.

3.2 Nozzle Noise and Uniformity Characterization with Hysteresis

In order to establish a baseline for future work within the ACE2.0 facility, a pitot survey was performed to measure and characterize the freestream noise and uniformity throuhgout the nozzle. Utilize pitot probe/rake and kulites mounted on traverse to characterize entire nozzle exit plane and centerline into nozzle up to 24??? inches upstream of nozzle exit.

Sweep Re/m and Mach to explore hysteresis of noise and maybe uniformity. Begin with Re/m sweep up and back down in current ACE.

The characterization test matrix is shown in Table ???. These runs are divided into a few distinct objectives: (1) uniformity, (2) uncerntainty, (3) pressure fluctiation transition, and (4) hysteresis.

The last seven runs will be replicates of the first seven to quantify the uncerntainty in pressure fluctuations, Mach number, and uniformity.

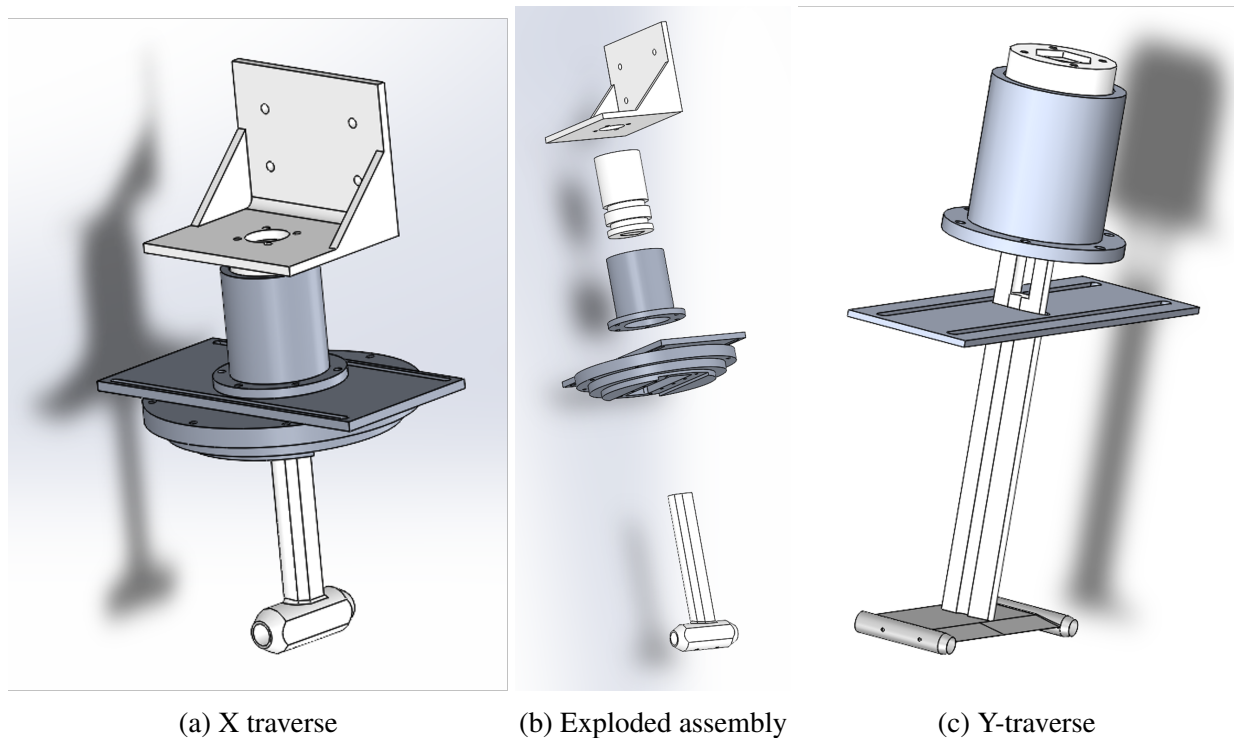


Figure 3.1: Traverse configurations

Run	X (in.)	Y (in.)	Z (in.)	Re/m ($\times 10^6$)
1	0	0	0	2→7→2
2	-17	0	0	2→7→2
3	-24	0	0	2→7→2

Table 3.1: Test matrix for preliminary noise hysteresis in ACE.

3.2.1 Uncerntainty Quantification

Reference [20]



Figure 3.2: Pitot probe measuring 17 in. upstream of nozzle exit.

3.2.2 Hysteresis

Stuff

3.3 Model Flow Characteristics Hysteresis During Mach Trajectory and Oscillation

This objective serves as a demonstration of capabilities for ACE2.0.

Look into hysteresis of boundary layers, shock interactions, and subsequent surface heat flux.

Use fin-cone model for public and HARV for army and verbal?

Run	X (in.)	Y (in.)	Z (in.)	Mach	Re/m ($\times 10^6$)
1	0	0	0	6	$2 \rightarrow 7 \rightarrow 2$
2	0	0	0	$5 \rightarrow 8 \rightarrow 5$	3
3	0	-3	-3:1:3	6	3
4	0	-1.5	-3:1:3	6	3
5	0	0	-3:1:3	6	3
6	0	1.5	-3:1:3	6	3
7	0	3	-3:1:3	6	3
8	-6	0	0	6	$2 \rightarrow 7 \rightarrow 2$
9	-6	0	0	$5 \rightarrow 8 \rightarrow 5$	3
10	-6	-3	-3:1:3	6	3
11	-6	-1.5	-3:1:3	6	3
12	-6	0	-3:1:3	6	3
13	-6	1.5	-3:1:3	6	3
14	-6	3	-3:1:3	6	3
15	-17	0	0	6	$2 \rightarrow 7 \rightarrow 2$
16	-17	0	0	$5 \rightarrow 8 \rightarrow 5$	3
17	-24	0	0	6	$2 \rightarrow 7 \rightarrow 2$
18	-24	0	0	$5 \rightarrow 8 \rightarrow 5$	3
19 (1)	0	0	0	6	$2 \rightarrow 7 \rightarrow 2$
20 (2)	0	0	0	$5 \rightarrow 8 \rightarrow 5$	3
21 (3)	0	-3	-3:1:3	6	3
22 (4)	0	-1.5	-3:1:3	6	3
23 (5)	0	0	-3:1:3	6	3
24 (6)	0	1.5	-3:1:3	6	3
25 (7)	0	3	-3:1:3	6	3

Table 3.2: Test matrix for ACE2.0 characterization and noise hysteresis study.

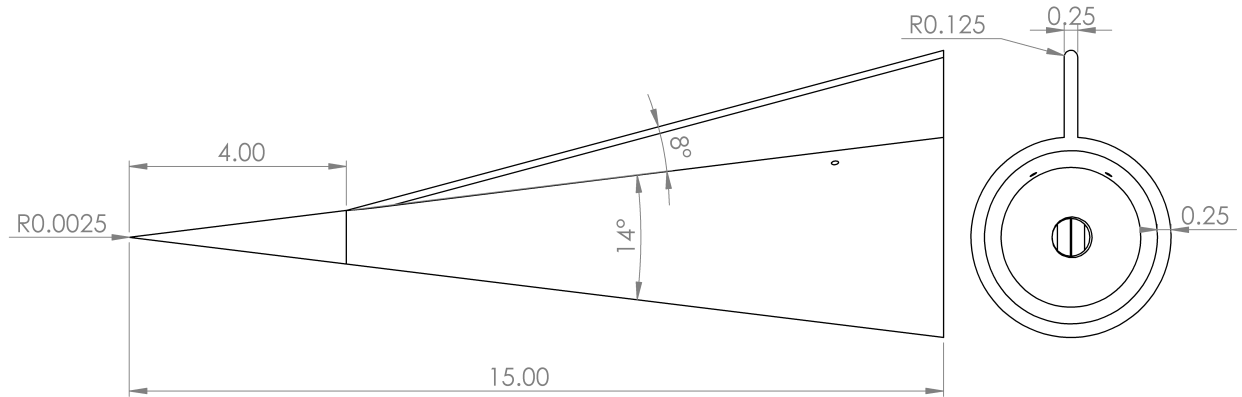


Figure 3.3: Drawing of 7° half-angle fin-cone model used for heat flux hysteresis study.

4. FUTURE WORK

Will do pressure test, program controls, final assembly, calibration, and finally experiments. A few objectives will be accomplished during the fabrication, install, and calibration.

Experiments and work in the following order:

1. Characterization of noise and uniformity throughout nozzle with hysteresis
2. Model BL, shock, and heating hysteresis
3. Constant/proportional Re/m controls if able

4.1 Maybe

Might have another section

4.2 Possibly

Could possibly have another section

REFERENCES

- [1] I. A. Leyva, “The relentless pursuit of hypersonic flight,” *Physics Today*, vol. 70, pp. 30–36, 11 2017.
- [2] J. T. Kenney and L. M. Webb, “A summary of the techniques of variable mach number supersonic wind tunnel nozzle design,” *AGARDograph*, no. 3, 1954.
- [3] J. Rosen, “The design and calibration of a variable mach number nozzle,” *Journal of the Aeronautical Sciences*, vol. 22, no. 7, pp. 484–490, 1955.
- [4] S. F. Erdmann, “A new economic flexible nozzle for supersonic wind tunnels,” *Journal of Aircraft*, vol. 8, no. 1, pp. 58–60, 1971.
- [5] J. Rom and I. Etsion, “Improved flexible supersonic wind-tunnel nozzle operated by a single jack.,” *AIAA Journal*, vol. 10, no. 12, pp. 1697–1699, 1972.
- [6] A. Durand, B. Chanetz, R. Benay, and A. Chpoun, “Investigation of shock waves interference and associated hysteresis effect at variable-mach-number upstream flow,” *Shock Waves*, vol. 12, p. 469–477, May 2003.
- [7] L. Laguarda, J. Santiago Patterson, F. F. Schrijer, B. W. van Oudheusden, and S. Hickel, “Experimental investigation of shock–shock interactions with variable inflow mach number,” *Shock Waves*, vol. 31, p. 457–468, Jul 2021.
- [8] P. Chen, F. Wu, J. Xu, X. Feng, and Q. Yang, “Design and implementation of rigid-flexible coupling for a half-flexible single jack nozzle,” *Chinese Journal of Aeronautics*, vol. 29, no. 6, pp. 1477–1483, 2016.
- [9] S.-g. Guo, Z.-g. Wang, and Y.-x. Zhao, “Design of a continuously variable mach-number nozzle,” *Journal of Central South University*, vol. 22, p. 522–528, Feb 2015.

- [10] Z. Lv, J. Xu, F. Wu, P. Chen, and J. Wang, “Design of a variable mach number wind tunnel nozzle operated by a single jack,” *Aerospace Science and Technology*, vol. 77, pp. 299–305, 2018.
- [11] W. Qi, J. Xu, and Z. Fan, *Design and Experimental Calibration of the Profile Rotating Wind Tunnel with Mach Number Varying from 2.0 to 4.0*.
- [12] C. A. Steeves, K. H. Timpano, P. T. Maxwell, L. Martinelli, and R. B. Miles, “Design and manufacture of a morphing structure for a shape-adaptive supersonic wind tunnel nozzle,” *Journal of Applied Mechanics*, vol. 76, no. 3, p. 031012, 2009.
- [13] D. Kraft, “Optimal control of a high performance wind tunnel,” *IFAC Proceedings Volumes*, vol. 18, no. 2, pp. 233–234, 1985. 5th IFAC Workshop on Control Applications of Nonlinear Programming and Optimization, Capri, Italy, Capri, Italy.
- [14] D.-S. Hwang and P.-L. Hsu, “A robust controller design for supersonic intermittent blowdown-type windtunnels,” *The Aeronautical Journal*, vol. 102, no. 1013, p. 161–170, 1998.
- [15] J. Matsumoto, F. Lu, and D. Wilson, “Pre-programmed controller for a supersonic blowdown tunnel,” 01 2001.
- [16] Y. T. Fung, G. Settles, and A. Ray, *Microprocessor Control of High-Speed Wind Tunnel Stagnation Pressure*.
- [17] B. Ilić, M. Miloš, and J. Isaković, “Cascade nonlinear feedforward-feedback control of stagnation pressure in a supersonic blowdown wind tunnel,” *Measurement*, vol. 95, pp. 424–438, 2017.
- [18] C. Nott, S. Ölçmen, D. Lewis, and K. Williams, “Supersonic, variable-throat, blow-down wind tunnel control using genetic algorithms, neural networks, and gain scheduled pid,” *Appl. Intell.*, vol. 29, pp. 79–89, 08 2008.

- [19] A. N. Shahrbabaki, M. Bazazzadeh, M. D. Manshadi, and A. Shahriari, “Designing a fuzzy logic controller for the reynolds number in a blowdown supersonic wind tunnel,” *2014 IEEE Aerospace Conference*, pp. 1–12, 2014.
- [20] J. Stephens, E. Hubbard, J. Walter, and T. McElroy, “Uncertainty analysis of the nasa glenn 8x6 supersonic wind tunnel,” tech. rep., 2016.
- [21] D. Curriston, *Uncerntainty*. Doctoral dissertation, Texas A&M University, 2024.
- [22] A. Chou, A. Leidy, R. A. King, B. F. Bathel, and G. Herring, *Measurements of Freestream Fluctuations in the NASA Langley 20-Inch Mach 6 Tunnel*.
- [23] L. Duan, M. M. Choudhari, A. Chou, F. Munoz, R. Radespiel, T. Schilden, W. Schröder, E. C. Marineau, K. M. Casper, R. S. Chaudhry, G. V. Candler, K. A. Gray, and S. P. Schneider, “Characterization of freestream disturbances in conventional hypersonic wind tunnels,” *Journal of Spacecraft and Rockets*, vol. 56, no. 2, pp. 357–368, 2019.
- [24] M. A. Kenworthy, *A Study of Unstable Axisymmetric Separation in High Speed Flows*. Virginia Polytechnic Institute and State University, 1978.
- [25] D. Beastall and J. Turner, “The effect of a spike protruding in front of a bluff body at supersonic speeds,” 1952.
- [26] A. Chpoun and G. Ben-Dor, “Numerical confirmation of the hysteresis phenomenon in the regular to the mach reflection transition in steady flows,” *Shock Waves*, vol. 5, pp. 199–203, 1995.
- [27] G. Ben-Dor, E. I. Vasiliev, T. Elperin, and A. Chpoun, “Hysteresis phenomena in the interaction process of conical shock waves: Experimental and numerical investigations,” *Journal of Fluid Mechanics*, vol. 448, p. 147–174, 2001.
- [28] M. Ivanov, G. Ben-Dor, T. Elperin, A. Kudryavtsev, and D. Khotyanovsky, “Flow-mach-number-variation-induced hysteresis in steady shock wave reflections,” *AIAA journal*, vol. 39, no. 5, pp. 972–974, 2001.

- [29] T. Setoguchi, S. Matsuo, M. Ashraful Alam, J. Nagao, and H. D. Kim, “Hysteretic phenomenon of shock wave in a supersonic nozzle,” *Journal of Thermal Science*, vol. 19, pp. 526–532, 2010.
- [30] Y. Tao, X. Fan, and Y. Zhao, “Viscous effects of shock reflection hysteresis in steady supersonic flows,” *Journal of fluid mechanics*, vol. 759, pp. 134–148, 2014.
- [31] J. M. Wirth, *Characterizing 3D Hypersonic Boundary Layers with Transient Surface Heat Flux Measurements*. PhD thesis, Texas A&M University, 2023.
- [32] M. Semper, N. Tichenor, R. Bowersox, R. Srinivasan, and S. North, *On the Design and Calibration of an Actively Controlled Expansion Hypersonic Wind Tunnel*.
- [33] N. Tichenor, M. Semper, R. Bowersox, R. Srinivasan, and S. North, *Calibration of an Actively Controlled Expansion Hypersonic Wind Tunnel*.
- [34] N. Tichenor, *Characterization of the Influence of a Favorable Pressure Gradient on the Basic Structure of a Mach 5.0 High Reynolds Number Supersonic Turbulent Boundary Layer*. Doctoral dissertation, Texas A&M University, 2010.
- [35] M. Semper, B. Pruski, and R. Bowersox, *Freestream Turbulence Measurements in a Continuously Variable Hypersonic Wind Tunnel*.
- [36] C. Mai, *Near-Region Modification of Total Pressure Fluctuations by a Normal Shock Wave in a Low-Density Hypersonic Wind Tunnel*. Doctoral dissertation, Texas A&M University, 2014.
- [37] I. Neel, *Influence of Environmental Disturbances on Hypersonic Crossflow Instability on the HIFiRE-5 Elliptic Cone*. Doctoral dissertation, Texas A&M University, 2019.
- [38] K. Sabnis, D. Galbraith, H. Babinsky, and J. A. Benek, *The Influence of Nozzle Geometry on Corner Flows in Supersonic Wind Tunnels*.
- [39] W. S. Saric, “Görtler vortices,” *Annual Review of Fluid Mechanics*, vol. 26, no. 1, pp. 379–409, 1994.

- [40] E. Reshotko, W. Saric, and H. Nagib, “Flow quality issues for large wind tunnels,” *35th Aerospace Sciences Meeting and Exhibit*, Jan 1997.
- [41] W. F. Hilton, “High speed wind tunnel testing. a. pope and k. l. goin. john wiley & sons, london. 1965. 474 pp. illustrations. 115s.” *The Aeronautical Journal*, vol. 70, no. 667, p. 739–739, 1966.
- [42] J. Anderson, *Fundamentals of Aerodynamics*. McGraw-Hill series in aeronautical and aerospace engineering, McGraw-Hill Education, 2017.
- [43] J. Anderson, *Modern Compressible Flow: With Historical Perspective*. Aeronautical and Aerospace Engineering Series, McGraw-Hill Education, 2021.

APPENDIX A

FIRST APPENDIX

Text for the Appendix follows.



Figure A.1: A caption here

APPENDIX B

APPENDIX 2

Text for the Appendix follows.



Figure B.1: A caption here

B.1 Appendix Section

B.2 Another Appendix Section